**Valorization of Cherry Pits: Great Lakes Agro-Industrial Waste to Mediate Great Lakes Water Quality**

Zoe A. Pollard and Jillian L. Goldfarb
Department of Biological and Environmental Engineering, Cornell University, 111 Wing Drive, Ithaca, NY, 14850, United States

**Prepared (by invitation) for submission to:** ***Environmental Pollution,*** Special issue on Biowaste Pollution from Agriculture, Forestry, Food Industry: Mitigation, Sustainable Utilization, Cleaner Disposal

**Abstract**

To meet human food and fiber needs in an environmentally and economically sustainable way, we must improve the efficiency of water and nutrient use by converting vast quantities of agricultural and food waste to renewable bioproducts. This work converts waste cherry pits, an abundant food waste in the Great Lakes region, to biochars and activated biochars via slow pyrolysis. Biochars produced have surface areas of 206-274 $m^2/g$ and increased bioavailability of Fe, K, Mg, Mn, and P increasing plant uptake of these nutrients and promoting root growth. The biochars can be implemented as soil amendments to reduce nutrient run-off and serve as a valuable carbon sink (biochars contain 74-79% carbon), potentially mitigating harmful algal blooms in the Great Lakes. The activated biochars have surface areas of up to 629 $m^2/g$ and exhibit selective metal adsorption for the removal of metals from drinking water sources, an environmental problem plaguing this region. Through sustainable waste-to-byproduct valorization we convert this waste food biomass into biochar for use as a soil amendment and into activated biochars to remove metals from drinking water, thus alleviating economic issues associated with cherry pit waste handling and reducing the environmental impact of the cherry processing industry.

**Keywords**: biochar, pyrolysis, water treatment, soil amendment

**Graphical Abstract:**

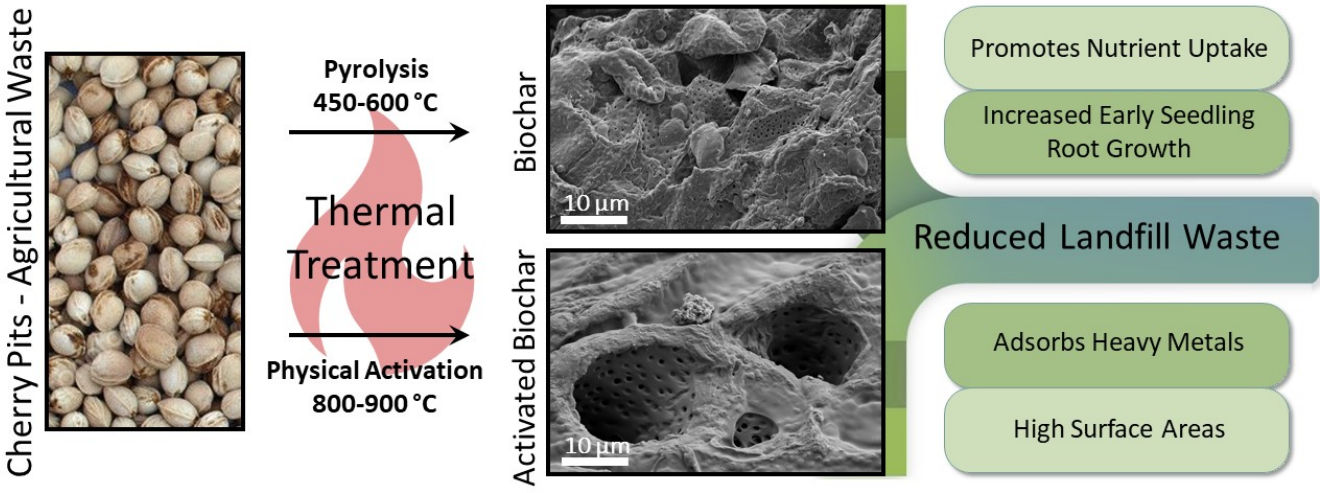

## 1 Introduction

The United States tart cherry industry faces wide-ranging challenges including increased competition from overseas imports, uncertainties associated with impacts due to climate change, and mounting organic landfill waste contributing to the methane footprint of agriculture. Tart cherry production in the United States totaled 329.3 million pounds in 2016 resulting in 40-50 million pounds of cherry pit byproduct waste[1]. Processing plants in the Great Lakes region handle 99 percent of the nation's cherries, separating the flesh for human consumption and underutilizing the pits as either direct soil amendments or for low yield craft projects, or just directly disposing of them in a landfill. Environmental concerns over biomass decomposition and the subsequent release of methane gas make direct soil amendments and landfill dumping inviable solutions to this agro-industrial waste problem[2]. Due to increasing production of tart cherries for food consumption, finding value-added applications for this abundantly available byproduct is an economic and environmental necessity.

While Great Lakes industries scramble to decrease their environmental footprint, the region also battles lake eutrophication and heavy metal contamination of drinking water. The Great Lakes region encompasses Lakes Superior, Michigan, Huron, Ontario, and Erie and this region has a high land use density of farming sites. Excess fertilizer runoff in this region leads to eutrophication of freshwater and increased nitrous oxide ($N_2O$) emissions, exacerbating climate change[3–5]. In addition to fertilizer runoff, a recent increase in erosion and dissolved reactive phosphorous has led to the re-eutrophication of Lake Erie, previously touted for its successful environmental cleanup[6,7]. The direct land application and/or composting of food and agricultural residues – including cherry pits – leads to decomposition of potentially valuable carbon sources[8–11] that increases nutrient run-off and greenhouse gas emissions[12].

In addition to contamination of natural waters, there is significant heavy metal contamination of drinking water in this region. Contaminants (including lead, barium, cadmium, selenium, arsenic, and chromium) enter drinking water through aging water transport infrastructure and groundwater contamination and lead to severe health effects[13]. A 2013 budget-guided decision to switch drinking water supplies from Detroit's system to the Flint River resulted in high lead contamination levels across Flint, Michigan. This was followed by a sharp increase in the amount of children with elevated blood lead levels[14]. Beyond Flint, arsenic levels in nearly 70% of Michigan's wells were found to exceed the United States Drinking Water standard of 10 μg/L[15]. Although the detrimental effects of these heavy metals on human health are well documented, the effectiveness and implementation of point-of-use-water filters requires further examination[16].

Given the proximity of cherry processing plants to such pressing environmental pollution, cherry pit biomass is a potential feedstock for conversion into water-remediating biochars. Biochars are a carbon rich solid material produced through pyrolysis, the thermochemical conversion of organic matter in an inert atmosphere[17]. As a soil amendment biochars can stabilize soil pH, reduce the need for fertilizer use, and decrease erosion risk[18]. The thermal conversion process increases the thermal stability of the carbon present in the material, this coupled with biochar addition to the soil effectively sequesters carbon in the soil. Biochar addition to soil is associated with decreased severity of nitrogen oxides ($NO_x$) and methane ($CH_4$) gas emissions from soils either by preventing the formation of these harmful greenhouse gasses and/or enhancing their oxidation after their formation[19].

Activated biochars produced through physical or chemical activation have increased porosity and surface area compared to raw biomass [20]. Physical activation involves the introduction of a porogen, typically steam or $CO_2$, during the thermal conversion process to open existing pores or generate new

micropores[21]. This activation method can recycle captured $CO_2$ from industrial gas streams[22] to further increase the environmental benefit of agricultural waste valorizations[23,24]. In addition, chemical activation requires high energy costs for drying after treatment and results in the handling and safe disposal of high quantities of hazardous chemical waste[25]. $CO_2$ activated biochars are known to be effective adsorbents for Pb(II)[26] and other heavy metals in contaminated water[27–30]. In this study, we employ pyrolysis (thermal decomposition in an inert atmosphere) and physical activation (partial gasification in a $CO_2$ atmosphere) to convert waste cherry pits into biochars and activated biochars.

There are a handful of studies concerning the valorization of tart cherry pits in recent years. Oils extracted from cherry pits have been recommended for use in cosmetics and cooking due to the presence of fatty acids[1]. Studies have demonstrated the potential to pyrolyze cherry pit waste to extract bio-oil as a renewable fuel[31], and others to co-fire the biomass with coal for electricity generation[32]. Others have proposed the use of cherry pit biochars as catalyst supports[33], electrode materials[34], alkaline-functionalized gas adsorbents[35], and as soil amendments to enhance greenhouse crop production[36]. In general, the transformation of biomass waste to biochars and activated carbons opens the possibilities of: (1) developing a revenue stream from an otherwise discarded waste; (2) enhancing nutrient use efficiency and soil stability; (3) mitigating drinking water pollution; (4) reducing anthropogenic environmental impacts of industrial food production. In the context of the Great Lakes Region, this biomass conversion would use a locally sourced waste to mediate local problems, reducing long-range transport of wastes and byproducts to improve environmental and human health of the local population.

## 2 Materials and Methods

United States tart cherries (*prunus cerasus*) were acquired from the Great Lakes Packing Company in Kewadin, MI. Preprocessing at the plant included drying in a large batch oven at 120 °C for 1 h then storage in a grain silo; cherry pits extracted over multiple seasons are stored together until the silo is full and the

pits are shipped to the landfill. The cherry pits received for this study are from the 2016-2018 harvest seasons. Upon receipt, cherry pits were rinsed in deionized water (DI $H_2O$) and dried on a benchtop at 22 °C. Cherry pits were mechanically ground and sieved to particle size ranges of 150-250 µm (Small) and 850-1100 µm (Large) then dried in an oven at 100 °C for 48 h. Subsequently the raw biomass was processed into biochars and activated biochars. The samples are named with the pyrolysis processing temperature, particle size abbreviation (S/L) and $CO_2$ activation is denoted with an A.

**2.1 Pyrolytic conversion of biomass to biochar**

To produce biochars, 3 g of processed biomass was placed in a porcelain boat in a fixed bed reactor (MTI single heating zone 2-inch GSL-1100X Tube Furnace) with nitrogen (>99%) flow at 100 mL/min. The samples were heated at 10 °C/min to 110 °C to dry for 30 min, then heated at the same rate to 450 °C or 600 °C and held for 60 min. The samples were cooled to ambient temperature under nitrogen. The resulting biochar was weighed, and biochar yield was calculated by dividing the final biochar mass by the initial biomass mass. The pyrolysis procedure was repeated three times at each condition; the solid yield was within 2% for each condition and the biochar from the repeated trials was combined for further analysis.

**2.2 $CO_2$ activation of biomass**

Samples were physically activated using $CO_2$ as a porogen. The ground and dried biomass was placed in a porcelain boat in the same MTI Tube furnace and heated at 10 °C/min under 100 mL/min of $N_2$ to 800 °C or 900 °C. Once at reaction temperature, the gas was switched to $CO_2$ at the same flowrate of 100 mL/min. Samples were held at the reaction temperature for 60 min, then allowed to cool to ambient temperature under $N_2$ to prevent oxidation.

**2.3 Characterization of resulting biochar and activated biochar**

Proximate analysis was performed on a TA Instruments Simultaneous Thermal Analyzer 650. 5 mg of sample was loaded into a 70 µL alumina crucible and heated at 50 °C/min under high purity $N_2$ (Airgas) at 100 mL/min to 110 °C. The sample was held at 110 °C for 30 min to remove moisture. The temperature was ramped up at 10 °C/min to 900 °C and held for 30 min to determine the percent of volatile matter present. Then the gas was switched to dry air at 100 mL/min and the temperature was increased to 950 °C at a rate of 10 °C/min to determine the percent of fixed carbon present. The resulting inorganic matter, loosely termed ash, was dissolved in 2% trace metal grade nitric acid for subsequent bioavailability calculations as described in Section 2.4. Ultimate analysis was performed to determine elemental carbon, hydrogen, nitrogen, and oxygen, with 2 mg of sample using a CE-440 Elemental Analyzer (Exeter Analytical, Inc.). Both proximate and ultimate analyses were conducted in triplicate, with averages and standard errors reported.

Surface area and pore volume were measured using $CO_2$ physisorption at 0 °C on a Micromeritics 3Flex Surface Area Analyzer over a $P/P_0$ range of 0 to 0.03. Specific surface areas were calculated using the Brunauer-Emmett-Teller (BET) method[37]. Prior to analysis samples were degassed at 150 °C for 16 h on a Micromeritics Smart VacPrep sample preparation device. Scanning electron microscopy (SEM) images of the uncoated raw biomass, biochars, and activated biochars were conducted using a LEO 1550 FESEM with an accelerating voltage of 3 kV. SEM images show surface features, textures, and pore structures of the samples.

pH and electrical conductivity were measured by equilibrating 0.2 g of sample in 4 mL Milli-Q water for 2 h. The samples were centrifuged, and the supernatant measured using a Mettler Toledo SevenExcellence Multiparameter probe with pH and electrical conductivity meters.

144

145 **2.4 Biochars as soil amendments**

146 A combination of Mehlich III[38] extraction and inorganic ash analysis was used to determine the percent
147 nutrient bioavailability for raw biomass and biochars. Available nutrient concentration was determined
148 via Mehlich III extraction using 0.01 g of each sample and 10 mL of Mehlich III extractant[39]. Extractant
149 from Mehlich III was digested in 70% trace metal grade nitric acid at 60 °C overnight then diluted to 2%
150 nitric acid using Milli-Q water. Total nutrient concentration was measured using the resulting ash from
151 proximate analysis. 0.05 mg ash was dissolved in 2% trace metal grade nitric acid. Inorganic nutrient
152 concentrations for the Mechlich III extractant and dissolved ash in 2% nitric acid were measured using a
153 Shimadzu Inductively Coupled Plasma Mass Spectrometry (ICP-MS-2030). Analysis was done in
154 quantitative mode using an internal standard with the collision cell activated for calcium and iron. The
155 percent nutrient bioavailability was calculated by Equation 1.

156 $$\%Bioavailability = \frac{[Nutrient\ available]}{[Total\ nurient]}\ x\ 100\% \quad (1)$$

157 Early seed growth in biochar amended soils was investigated by germinating Arugula (*eruca vesicaria*)
158 seeds in 2 g Sungro Black Gold All-purpose potting mix with 5 wt% biochar or biomass for 7 days[40]. 10
159 seeds were planted in each biochar amended soil and unamended soil, as a control. Plant stalk and root
160 lengths were measured. The resulting sprouts were brushed free of soil, weighed, rinsed in DI water, and
161 dried. The dried arugula sprouts were digested in 70% trace metal grade nitric acid at 60 °C overnight then
162 diluted to 2% nitric acid using Milli-Q water. The resulting solution was analyzed via ICP-MS using an
163 internal standard to determine the concentrations of heavy metals and nutrients.

164

165 Potential carcinogen and toxicants present in the biochars were determined via Soxhlet extraction run for
166 48 h using 100 mL of 1:1 mixed solvent of acetone to hexanes, 0.5 g biochar sample and 0.1 g anhydrous

sodium sulfate as described in EPA method 3540C[41]. Extractant was dewatered with anhydrous magnesium sulfate then analyzed using a Shimadzu Single Quadrupole Gas Chromatograph-Mass Spectrometer (GCMS-QP2020). The initial column oven temperature was 40 °C with an injection temperature of 250 °C and a split ratio of 1:1. After 5 min the oven temperature was increased 1.25 °C/min to 150 °C and held for 5 min. The oven temperature was then increased 1.50 °C/min to 250 °C and held for 10 min. The mass spectrometer scanned from 15 to 500 M/Z and data was recorded after a solvent cut time of 6 min.

**2.5 Activated biochars for water treatment**

To investigate qualitative changes in surface functional groups upon physical activation of the cherry pits, Fourier transform infrared spectroscopy was performed on a series of samples using a Bruker Vertex 70 Fourier Transform Infrared Spectrometer (FT-IR) over a wavenumber range of 4000 – 400 $cm^{-1}$ using KBr discs containing 2% finely ground biochar sample. Spectra were baseline corrected and normalized to the O-H band.

To gauge the potential of the activated carbons to adsorb metals from drinking water, two metal solutions were prepared. The first containing Co, Cu, Ni, Mn, and Zn at 50 ppm in Milli-Q water (Solution 1 - S1), the second Primary Drinking Water Metal Solution (High Purity Standards) was used to simulate contaminated drinking water and includes Ag 10 ppm, As 100 ppm, Ba 50 ppm, Cd 50 ppm, Cr 100 ppm, Pb 100 ppm, and Se 50 ppm diluted to 50 ppm Pb with Milli-Q water (Solution 2 - S2). Kinetics experiments were conducted using 0.05 g activated biochar or raw sample in 12 mL of solution with 0.5 mL of water withdrawn at each measurement point. Equilibrium was established after 16 h. Metal concentrations were measured using the Shimadzu ICP-MS with an internal standard, and the adsorption capacity of each metal was calculated.

## 3 Results and Discussion:

Biochar yields ranged from 28-31% and dropped to 24% and 14% for activated biochars at 800 °C and 900 °C, respectively. This drop in yield due to treatment at higher temperatures with a $CO_2$ activating agent results in increased devolatilization and oxidation leading to more mass loss. A summary of characterizations of biomass, biochar, and activated biochar is shown in Table 1. Larger particle sizes and increased pyrolysis temperatures formed biochars with an increased BET surface area, as determined by $CO_2$ physisorption. An activation temperature of 900 °C developed more micropores[42] and produced the char with the largest surface area of 629 $m^2/g$. This is 30% higher than previously reported literature values of 485 $m^2/g$ for cherry pits chemically activated using $H_2SO_4$[20].

**Table 1.** Porosity, pH, electrical conductivity, and biochar yield of raw biomass, biochar, and activated biochar.

| | BET Surface Area ($m^2/g$) | Total Pore Volume (cc/g) | pH | Electrical Conductivity (mS/cm) | Biochar Yield (wt %) |
|---|---|---|---|---|---|
| Raw-S | n.d. | n.d. | 4.8 | 1071 | n.d. |
| Raw-L | n.d. | n.d. | 5.7 | 344 | n.d. |
| 450-S | 206.8 ± 0.4 | 0.0606 | 10.2 | 439 | 31.3 ± 0.4 |
| 450-L | 220.9 ± 0.4 | 0.0663 | 8.5 | 187 | 28.2 ± 0.8 |
| 600-S | 254.0 ± 0.3 | 0.0924 | 10.0 | 788 | 28.8 ± 0.1 |
| 600-L | 274.4 ± 0.5 | 0.0923 | 9.2 | 315 | 29.8 ± 1.6 |
| 800-Activated | 352.7 ± 4.0 | 0.1265 | 11.1 | 1080 | 24.0 ± 0.2 |
| 900-Activated | 629.8 ± 1.9 | 0.1200 | 10.5 | 1545 | 14.6 ± 0.2 |

* 2- column fitting image

### 3.1 Application of biochars as soil amendments

To utilize cherry pit biochars as soil amendments the soil properties must be considered as well as the effect on plant growth. Key properties of the soil that are accounted for are pH, electrical conductivity (Table 1), and potential toxicity. Potential toxicant and carcinogens, including the IBI priority polycyclic aromatic hydrocarbons[43] were not detected by Soxhlet extraction and GC-MS analysis in any sample. Chromatograms are reported in Supplemental Materials Figure S1.

**Table 2.** Proximate and Ultimate analysis of raw biomass and biochars. Ultimate analysis results are reported on an ash free basis.

| | Proximate Analysis (dry basis wt %) | | | Ultimate Analysis | | | |
|---|---|---|---|---|---|---|---|
| | Volatile Matter | Fixed Carbon | Ash | Carbon (%) | Hydrogen (%) | Nitrogen (%) | Oxygen[a] (%) |
| Raw-S | 80.7 ± 0.0 | 16.0 ± 0.0 | 3.3 ± 0.1 | 51.9 ± 0.0 | 7.6 ± 0.0 | 3.8 ± 0.0 | 36.7 ± 0.1 |
| Raw-L | 77.7 ± 0.1 | 22.3 ± 0.0 | 0.0 ± 0.1 | 51.6 ± 0.1 | 6.8 ± 0.0 | 0.3 ± 0.0 | 41.2 ± 0.1 |
| 450-S | 16.1 ± 0.1 | 75.8 ± 4.6 | 8.1 ± 4.5 | 74.5 ± 0.1 | 3.2 ± 0.0 | 4.0 ± 0.1 | 18.3 ± 0.0 |
| 450-L | 15.8 ± 0.0 | 84.2 ± 0.1 | 0.0 ± 0.0 | 75.3 ± 1.5 | 3.2 ± 0.1 | 3.3 ± 0.8 | 20.5 ± 0.8 |
| 600-S | 10.2 ± 0.3 | 86.0 ± 2.3 | 3.9 ± 2.6 | 78.5 ± 0.0 | 2.1 ± 0.0 | 3.7 ± 0.0 | 15.7 ± 0.0 |
| 600-L | 8.5 ± 0.2 | 84.7 ± 0.9 | 6.8 ± 0.8 | 78.7 ± 0.4 | 2.4 ± 0.0 | 2.3 ± 0.1 | 16.6 ± 0.2 |
| 800-A | 5.2 ± 0.1 | 90.7 ± 0.6 | 4.1 ± 0.7 | 78.3 ± 0.0 | 1.2 ± 0.0 | 2.4 ± 0.0 | 18.1 ± 0.0 |
| 900-A | 5.2 ± 0.1 | 78.9 ± 0.4 | 15.9 ± 0.3 | 76.3 ± 0.0 | 0.5 ± 0.0 | 0.4 ± 0.0 | 22.9 ± 0.0 |

[a]Oxygen calculated by difference.

* 2- column fitting image

Proximate analysis of both untreated and pyrolyzed cherry pits was performed to determine the stability of the carbon present before and after treatment (Table 2). Both large and small sized raw cherry pits comprised >77% volatile matter (VM), while all pyrolyzed samples had <17% VM. This is expected given that pyrolysis devolatilizes volatile matter, leaving a more carbonaceous (graphitic) solid with proportionately higher fixed carbon and ash contents, but elementally less hydrogen and oxygen. Ultimate analysis results show the elemental carbon concentration increasing from 51% for the raw biomass to 74-79% with thermal conversion. Pyrolysis at lower temperatures generates more biochar and requires lower energy input while still producing a high carbon content product for effective carbon sequestration[44].

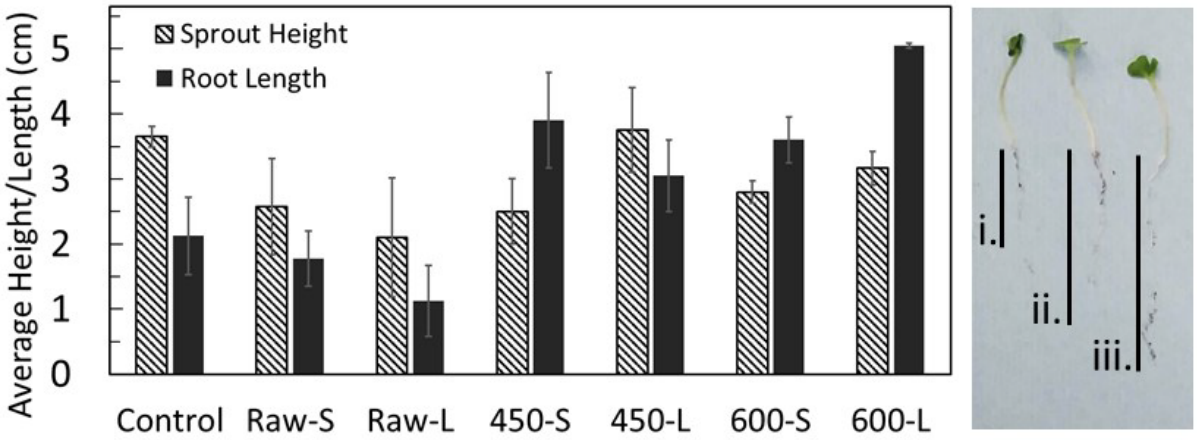


Figure 2. Left: Average sprout height and root length for arugula sprouts grown in control soil, and soil amended with raw biomass, and biochars. Right: Examples of sprouts in soil amended with i. Raw S, ii. 450 S, and iii. 600 L, black bars represent root length.
* 2- column fitting image

Next, the performance of biochar as a soil amendment was studied via germination tests with arugula seeds. The sprout height and root lengths after one week of growth are provided in Figure 2; germination was successful for all seeds planted. The arugula sprouts grown in soil containing biochars had, on average, 1.8 times longer roots than those in control soils and 2.7 times longer roots than those grown in

235 the presence of raw biomass. Three representative sprouts in Figure 2 show the consistency in sprout
236 height and increase in average root length.
237
238 As shown in Table 3, thermal treatment of the biomass led to an increase in the bioavailable Fe, K, Mg,
239 Mn, and P, as well as a decrease in extractable Se and Zn. Nutrient bioavailability, apart from Se for
240 biochars at 600 °C, is higher for small particle sized samples due to higher accessibility of internal bulk
241 material. To probe the implications of increased bioavailability in the biochars, the nutrient and heavy
242 metal concentrations in the sprouts grown in amended soils were measured (available in SI). Sprouts
243 grown in soils with more aggressively treated biochars (higher pyrolysis temperatures) had decreased
244 concentrations of toxic metals such as As, Be, Cd, Co, In, Pb, and Tl. Arugula grown in biochar amended
245 soil exhibited higher concentrations of key nutrients including K, Mg, Mn, and P, which can be attributed
246 to their increased bioavailability in the biochar.
247
248 Table 3. Percent nutrient bioavailability for raw biomass and biochars. The standard deviation for all
249 %Bioavailability measurements is <2%.

| | Bioavailability (%) | | | | | | | |
|---|---|---|---|---|---|---|---|---|
| Sample | Al | Fe | K | Mg | Mn | P | Se | Zn |
| Raw-S | 24 | 27 | 15 | 31 | 22 | 38 | 36 | 13 |
| Raw-L | 9.0 | 16 | 2.0 | 4.9 | 11 | 8.2 | 28 | 9.5 |
| 450-S | 27 | 73 | 24 | 91 | 98 | 93 | 10 | 4.6 |
| 450-L | 22 | 43 | 12 | 60 | 85 | 59 | 8.6 | 3.1 |
| 600-S | 22 | 48 | 25 | 66 | 96 | 78 | 6.4 | 3.9 |
| 600-L | 18 | 36 | 27 | 53 | 92 | 56 | 8.1 | 3.1 |

250 * single- column fitting image
251
252 The raw biomass is slightly acidic whereas the biochars and activated biochars are slightly alkaline (Table
253 1). pH values are consistent with reported biochar soil amendments[45] although effects of biochar addition
254 on soil pH and conductivity are dependent on the properties of the particular soil[46]. Previous studies have
255 reported increases in soil pH due to the addition of basic biochar are associated with increased uptake of

nutrients including K and P[47], and decreased mobility of metals in the soil[48]. Increased bioavailability of these nutrients and uptake by crops decreases the chance of nutrients leaching into local water sources and nearby lakes[49]. The results of this are twofold: 1) a reduced need for fertilizers and other nutrient additives in decreasing material costs in farming and 2) decreased nutrient runoff into the Great Lakes, potentially improving water quality.

### 3.2 Application of activated biochars for water treatments

Cherry pit activated biochars with high surface areas were produced using $CO_2$ physical activation at 800 °C and 900 °C. In addition to the high surface areas of the activated biochars, the adsorption properties of the activated biochars were investigated. Proximate analysis reveals the cherry pit activated biochars both contain 5.2% VM (Table 2). 800-A contains 90.7% fixed carbon and 4.1% inorganic matter. 900-A experienced partial decomposition of the fixed carbon resulting in 78.9% fixed carbon and 15.9% inorganic matter. Ultimate analysis of the activated biochar results show elemental carbon consistent between the activated and inactivated biochars (Table 2). Elemental hydrogen and nitrogen decreased with increasing processing temperatures[50].

SEM images show the textural details of the surface of raw cherry pit biomass, activated biochars at 800 °C and 900 °C (Figure 3A). Raw cherry pits have high density and uniformity compared to the well-structured porous nature of the 800 °C activated biochars and the fragile highly porous 900 °C activated biochars. These results show qualitative evidence for the effectiveness of the physical activation and the resulting increase in surface area and pore volume.

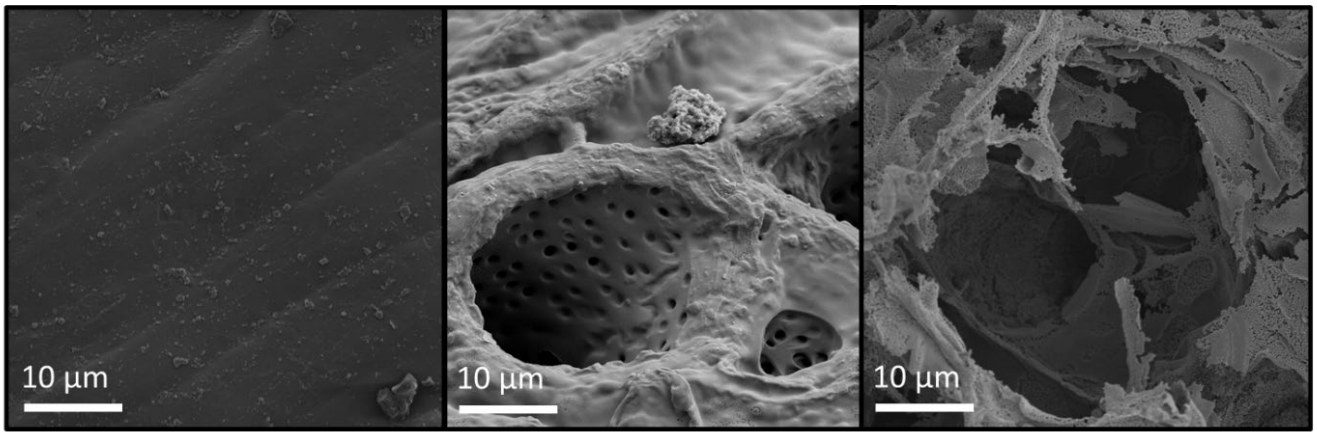


A. SEM images of raw cherry pit and activated carbons at 800 °C and 900 °C

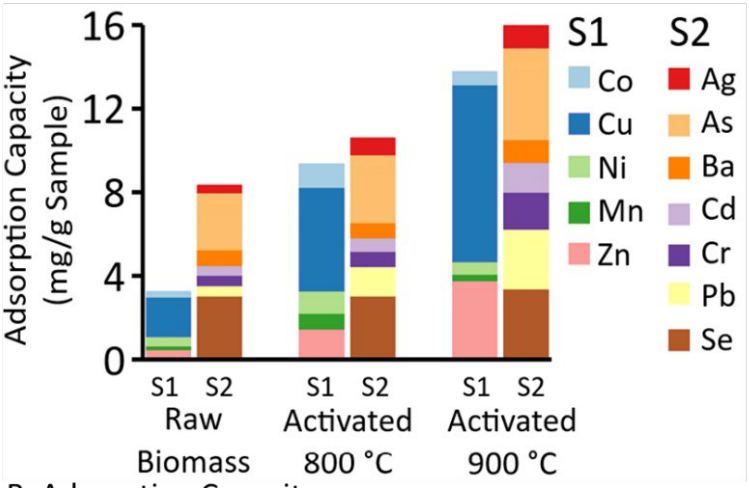


B. Adsorption Capacity

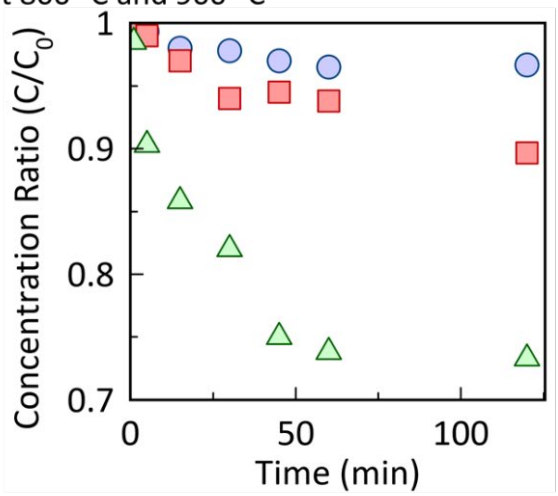


C. Cu Adsorption Kinetics

Figure 3. A. Surface features shown via SEM, B. adsorption capacity for each sample by element in Solution 1 (S1) and Solution 2 (S2), and C. representative copper adsorption kinetics results for raw biomass ( ○ blue circle) and activated biochars with peak pyrolysis temperatures of 800 °C ( □ red square) and 900 °C ( △ green triangle).
* 2- column fitting image

High surface areas are often associated with higher adsorption capacities (though prior work has demonstrated that this is not always the case[51]). Adsorption capacities from Solution 1 and Solution 2 are shown in Figure 3B. The adsorption capacity of Cu in Solution 1 on the activated biochars at 900 °C was 8.48 milligram Cu per gram of activated biochar, shown in Figure 3C. In Solution 1, physical activation increased the total metal adsorbed by 2.8 and 4.2 times for the activated biochars at 800 °C and 900 °C, respectively, as compared to the raw cherry pit biochars. Similarly, in Solution 2, total metal adsorption was increased by 1.2 and 1.9 times for the activated biochars at 800 °C and 900 °C,

respectively. Activated biochars show high affinity for copper and zinc in Solution 1 and arsenic and lead in Solution 2 which is representative of a contaminated water sourced from municipal waters in the Unites States. Complete adsorption results for all metals is provided in Supplemental Information Table S2. The increased adsorption capacity of biochars after activation is ideal for heavy metal removal from drinking water.

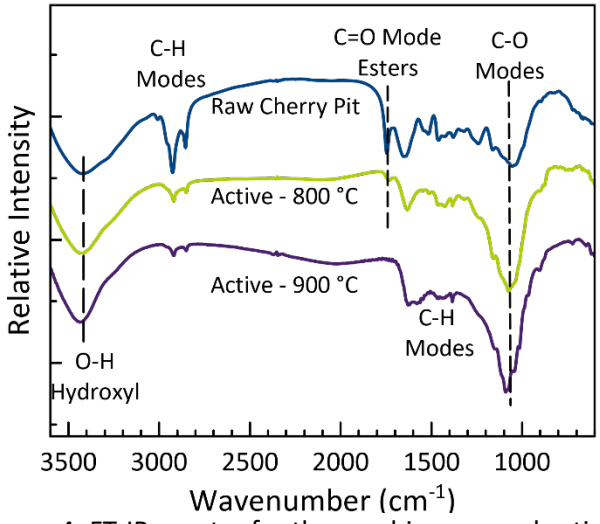


Figure 4: FT-IR spectra for the raw biomass and activated biochars.
* single- column fitting image

FTIR was performed to characterize the surface functional groups, as shown in Figure 4. A relative decrease in C-H bands centered at 2926 $cm^{-1}$ and 2854 $cm^{-1}$ was found after thermal treatment and activation of the biochars. Esters were identified at 1745 $cm^{-1}$ for the raw biomass, with an 85% reduction for the 800 °C activated biochars, and were not detected for the 900 °C activated biochars. Thermal treatment increased the area of peaks asociated with C-O ether and alchohol modes in the 1000-1150 $cm^{-1}$ range but resulted in a loss of methyl and ester bands, which is consistant with more hydrophillic biochar surface due to the higher density ratio of hydroxyl species relative to the hydrophobic methyl chains. The increased adsorption capacity of 900-A compared to 800-A and the raw biomass can be attributed to this increase in surface hydrophilicity, which in turn increases the metal adsorption affinity of the activated biochar[52].

This work highlights the conversion of waste cherry pits to biochars and activated biochars. As soil amendments the biochars showed low metal bioavailability and high nutrient bioavailability, promoting the uptake of nutrients and increasing root growth. As activated biochars, surface areas higher than those previously reported were achieved resulting in materials with high metal adsorption potential. Agricultural waste is an abundant and inexpensive carbonaceous feedstock[53] and further investigation is necessary into the conversion of local waste streams into value added products for the treatment of environmental tragedies. Expansion of this work should include the development of processing pathways for agricultural wastes with high density processing plants throughout the nation, such as corn stover and cow manure. These biomasses serve as viable feedstocks for conversion to biochar and further investigation is necessary into the application of these converted materials to address environmental contaminations surrounding the specific waste generation sites[54]. A full analysis surrounding the potential for creating a circular carbon economy where waste carbonaceous materials are not allowed decompose and generate pollution, but instead aid in environmental cleanup efforts[55,56].

## 4 Conclusions

As an abundant waste biomass near the source of water contamination in the Great Lakes region, cherry pits represent a viable feedstock for conversion to biochars and activated biochars for soil amendments and heavy metal removal from drinking water, respectively, addressing two critical regional challenges. Biochars and activated biochars were produced via pyrolysis and physical activation using $CO_2$. Thermal processing preserved large amounts of the carbon, effectively sequestering carbon when used as a soil amendment. Cherry pit biochars enhanced root growth in limited sprouting applications and increased the uptake of essential nutrients while decreasing the uptake and mobility of undesirable metals. Surface areas of up to 629 $m^2/g$ were achieved for the activated biochars and the total metal adsorbed increased

by 4.2 and 1.9 times for the activated biochars at 900 °C for Solution 1 and Solution 2, respectively, as compared to the raw cherry pit biochars. The continuing success of agricultural industries in the United States, including the tart cherry industry, requires a shift away from traditional waste disposal towards a reallocation of these materials to greener sources of biomass to produce materials for water treatments.

**Acknowledgments**

This research was supported by the Arthur Boller Research Grant and the National Science Foundation through CMMI grant 1727316. This work used the Cornell Center for Materials Research Shared Facilities which are supported through the NSF MRSEC program (DMR-1719875).

**References**

(1) Korlesky, N. M.; Lucas, ·; Stolp, J.; Dharma, ·; Kodali, R.; Goldschmidt, · Robert; William, ·; Byrdwell, C. Extraction and Characterization of Montmorency Sour Cherry (Prunus Cerasus L.) Pit Oil. *J Am Oil Chem Soc* **2016**, *93*, 995–1005. https://doi.org/10.1007/s11746-016-2835-4.

(2) Kučić, D.; Kopčić, N.; Briški, F. Biodegradation of Agro-Industrial Waste. *Chem. Biochem. Eng. Q* **2017**, *31* (4), 369–374. https://doi.org/10.15255/CABEQ.2017.1116.

(3) Sharpley, A.; Foy, B.; Withers, P. Practical and Innovative Measures for the Control of Agricultural Phosphorus Losses to Water: An Overview. *J. Environ. Qual.* **2000**, *29* (1), 1. https://doi.org/10.2134/jeq2000.00472425002900010001x.

(4) Johansson, K.; Perzon, M.; Fröling, M.; Mossakowska, A.; Svanström, M. Sewage Sludge Handling with Phosphorus Utilization - Life Cycle Assessment of Four Alternatives. *J. Clean. Prod.* **2008**, *16* (1), 135–151. https://doi.org/10.1016/j.jclepro.2006.12.004.

(5) Cassman, K. G.; Dobermann, A.; Walters, D. T.; Yang, H. Meeting Cereal Demand While Protecting Natural Resources and Improving Environmental Quality. *Annu. Rev. Environ. Resour.* **2003**, *28* (1), 315–358. https://doi.org/10.1146/annurev.energy.28.040202.122858.

(6) Baker, D. B.; Confesor, R.; Ewing, D. E.; Johnson, L. T.; Kramer, J. W.; Merryfield, B. J. Phosphorus Loading to Lake Erie from the Maumee, Sandusky and Cuyahoga Rivers: The Importance of

Bioavailability. **2014**. https://doi.org/10.1016/j.jglr.2014.05.001.

(7) Keitzer, S. C.; Ludsin, S. A.; Sowa, S. P.; Annis, G.; Arnold, J. G.; Daggupati, P.; Froehlich, A. M.; Herbert, M. E.; Johnson, M. V. V.; Sasson, A. M.; et al. Thinking Outside of the Lake: Can Controls on Nutrient Inputs into Lake Erie Benefit Stream Conservation in Its Watershed? *J. Great Lakes Res.* **2016**, *42* (6), 1322–1331. https://doi.org/10.1016/j.jglr.2016.05.012.

(8) Camargo, G. G. T.; Ryan, M. R.; Richard, T. O. M. L. Energy Use and Greenhouse Gas Emissions from Crop Production Using the Farm Energy Analysis Tool. *Bioscience* **2013**, *63* (4), 263–273. https://doi.org/10.1525/bio.2013.63.4.6.

(9) Hao, X.; Chang, C.; Larney, F. J.; Travis, G. R. Greenhouse Gas Emissions during Cattle Feedlot Manure Composting. *J. Environ. Qual.* **2001**, *30* (2), 376. https://doi.org/10.2134/jeq2001.302376x.

(10) Capper, J. L. The Environmental Impact of Beef Production in the United States: 1977 Compared with 2007. *J. Anim. Sci.* **2011**, *89* (12), 4249–4261. https://doi.org/10.2527/jas.2010-3784.

(11) Koneswaran, G.; Nierenberg, D.; Farm, G.; Production, A.; Change, M. C. Global Farm Animal Production and Global Warming : Impacting and Mitigating Climate Change. *Environ. Health Perspect.* **2008**, *116* (5), 578–582. https://doi.org/10.1289/ehp.ll034.

(12) Sánchez, A.; Artola, A.; Font, X.; Gea, T.; Barrena, R.; Gabriel, D.; Sánchez-Monedero, M. Á.; Roig, A.; Cayuela, M. L.; Mondini, C. Greenhouse Gas from Organic Waste Composting: Emissions and Measurement; Springer, Cham, 2015; pp 33–70. https://doi.org/10.1007/978-3-319-11906-9_2.

(13) Tchounwou, P. B.; Yedjou, C. G.; Patlolla, A. K.; Sutton, D. J. Heavy Metals Toxicity and the Environment. *Mol. Clin. Environ. Toxicol.* **2012**, 133–164. https://doi.org/10.1007/978-3-7643-8340-4_6.

(14) Abokifa, A. A.; Katz, L.; Sela, L. Spatiotemporal Trends of Recovery from Lead Contamination in Flint, MI as Revealed by Crowdsourced Water Sampling. **2019**.

https://doi.org/10.1016/j.watres.2019.115442.

(15) Kolker, A.; Haack, S. K.; Cannon, W. F.; Westjohn, D. B.; Kim, M.-J.; Nriagu, J.; Woodruff, L. G. Arsenic in Southeastern Michigan. In *Arsenic in Ground Water*; Kluwer Academic Publishers, 2005; pp 281–294. https://doi.org/10.1007/0-306-47956-7_10.

(16) Slotnick, M. J.; Meliker, J. R.; Nriagu, J. O. Effects of Time and Point-of-Use Devices on Arsenic Levels in Southeastern Michigan Drinking Water, USA. **2006**. https://doi.org/10.1016/j.scitotenv.2006.04.021.

(17) Lam, S. S.; Lee, X. Y.; Nam, W. L.; Phang, X. Y.; Liew, R. K.; Yek, P. N. Y.; Ho, Y. L.; Ma, N. L.; Rosli, M. H. N. B. Microwave Vacuum Pyrolysis Conversion of Waste Mushroom Substrate into Biochar for Use as Growth Medium in Mushroom Cultivation. *J. Chem. Technol. Biotechnol.* **2019**, *94* (5), 1406–1415. https://doi.org/10.1002/jctb.5897.

(18) Lehmann, J. A Handful of Carbon. *Nature*. Nature Publishing Group May 10, 2007, pp 143–144. https://doi.org/10.1038/447143a.

(19) Johannes Lehmann. Bio-Energy in the Black. *Front. Ecol. Environ.* **2007**, *5* (September), 381–387.

(20) Gheju, M.; Balcu, I.; Jurchescu, P. Removal of Hexavalent Chromium from Aqueous Solutions by Use of Chemically Modified Sour Cherry Stones. *Desalin. Water Treat.* **2016**, *57* (23), 10776–10789. https://doi.org/10.1080/19443994.2015.1040468.

(21) Liew, R. K.; Chong, M. Y.; Osazuwa, O. U.; Nam, W. L.; Phang, X. Y.; Su, M. H.; Cheng, C. K.; Chong, C. T.; Lam, S. S. Production of Activated Carbon as Catalyst Support by Microwave Pyrolysis of Palm Kernel Shell: A Comparative Study of Chemical versus Physical Activation. *Res. Chem. Intermed.* **2018**, *44* (6), 3849–3865. https://doi.org/10.1007/s11164-018-3388-y.

(22) Mikulčić, H.; Ridjan Skov, I.; Dominković, D. F.; Wan Alwi, S. R.; Manan, Z. A.; Tan, R.; Duić, N.; Hidayah Mohamad, S. N.; Wang, X. Flexible Carbon Capture and Utilization Technologies in Future Energy Systems and the Utilization Pathways of Captured CO2. *Renew. Sustain. Energy*

*Rev.* **2019**, *114*, 109338. https://doi.org/10.1016/j.rser.2019.109338.

(23) Nai Yuh Yek, P.; Peng, W.; Chung Wong, C.; Keey Liew, R.; Ling Ho, Y.; Adibah Wan Mahari, W.; Azwar, E.; Qi Yuan, T.; Tabatabaei, M.; Aghbashlo, M.; et al. Engineered Biochar via Microwave CO 2 and Steam Pyrolysis to Treat Carcinogenic Congo Red Dye. **2020**. https://doi.org/10.1016/j.jhazmat.2020.122636.

(24) Li, Y.; Liu, J.; Yuan, Q.; Tang, H.; Yu, F.; Lv, X. A Green Adsorbent Derived from Banana Peel for Highly Effective Removal of Heavy Metal Ions from Water. *RSC Adv.* **2016**, *6* (51), 45041–45048. https://doi.org/10.1039/c6ra07460j.

(25) Ukanwa, K. S.; Patchigolla, K.; Sakrabani, R.; Anthony, E.; Mandavgane, S. A Review of Chemicals to Produce Activated Carbon from Agricultural Waste Biomass. *Sustain.* **2019**, *11* (22), 1–35. https://doi.org/10.3390/su11226204.

(26) N, Z.; H, C.; J, X.; D, Y.; Z, Z.; Y, T.; X, L. Biochars with Excellent Pb(II) Adsorption Property Produced from Fresh and Dehydrated Banana Peels via Hydrothermal Carbonization. *Bioresour. Technol.* **2017**, *232*, 204–210.

(27) Dou, G.; Goldfarb, J. In Situ Upgrading of Pyrolysis Biofuels by Bentonite Clay with Simultaneous Production of Heterogeneous Adsorbents for Water Treatment. *Fuel* **2017**, *195*, 273–283. https://doi.org/10.1016/j.fuel.2017.01.052.

(28) Gopu, C.; Gao, L.; Volpe, M.; Fiori, L.; Goldfarb, J. L. Valorizing Municipal Solid Waste: Waste to Energy and Activated Carbons for Water Treatment via Pyrolysis. *J. Anal. Appl. Pyrolysis* **2018**. https://doi.org/10.1016/j.jaap.2018.05.002.

(29) Mohan, D.; Sarswat, A.; Ok, Y. S.; Pittman, C. U. Organic and Inorganic Contaminants Removal from Water with Biochar, a Renewable, Low Cost and Sustainable Adsorbent - A Critical Review. *Bioresour. Technol.* **2014**, *160* (February 2014), 191–202. https://doi.org/10.1016/j.biortech.2014.01.120.

(30) Goldfarb, J. L.; Buessing, L.; Gunn, E.; Lever, M.; Billias, A.; Casoliba, E.; Schievano, A.; Adani, F. Novel Integrated Biorefinery for Olive Mill Waste Management: Utilization of Secondary Waste for Water Treatment. *ACS Sustain. Chem. Eng.* **2017**, *5* (1), 876–884. https://doi.org/10.1021/acssuschemeng.6b02202.

(31) Duman, G.; Okutucu, C.; Ucar, S.; Stahl, R.; Yanik, J. The Slow and Fast Pyrolysis of Cherry Seed. *Bioresour. Technol.* **2011**, *102* (2), 1869–1878. https://doi.org/10.1016/j.biortech.2010.07.051.

(32) Yangali, P.; Celaya, A. M. A. A. M.; Goldfarb, J. J. L. Co-Pyrolysis Reaction Rates and Activation Energies of West Virginia Coal and Cherry Pit Blends. *J. Anal. Appl. Pyrolysis* **2014**, *108*, 203–211. https://doi.org/10.1016/j.jaap.2014.04.015.

(33) Li, X.; Tie, K.; Li, Z.; Guo, Y.; Liu, Z.; Liu, X.; Liu, X.; Feng, H.; Zhao, X. S. Nitrogen-Doped Hierarchically Porous Carbon Derived from Cherry Stone as a Catalyst Support for Purification of Terephthalic Acid. *Appl. Surf. Sci.* **2018**, *447*, 57–62. https://doi.org/10.1016/j.apsusc.2018.03.195.

(34) Hernández-Rentero, C.; Córdoba, R.; Moreno, N.; Caballero, A.; Morales, J.; Olivares-Marín, M.; Gómez-Serrano, V. Low-Cost Disordered Carbons for Li/S Batteries: A High-Performance Carbon with Dual Porosity Derived from Cherry Pits. *Nano Res.* **2018**, *11* (1), 89–100. https://doi.org/10.1007/s12274-017-1608-1.

(35) Savova, D.; Apak, E.; Ekinci, E.; Yardim, F.; Petrov, N.; Budinova, T.; Razvigorova, M.; Minkova, V. Biomass Conversion to Carbon Adsorbents and Gas. *Biomass and Bioenergy* **2001**, *21* (2), 133–142. https://doi.org/10.1016/S0961-9534(01)00027-7.

(36) Barber, S. T.; Yin, J.; Draper, K.; Trabold, T. A. Closing Nutrient Cycles with Biochar- from Filtration to Fertilizer. *J. Clean. Prod.* **2018**, *197*, 1597–1606. https://doi.org/10.1016/j.jclepro.2018.06.136.

(37) Brunauer, S.; Emmett, P. H.; Teller, E. Adsorption of Gases in Multimolecular Layers. *J. Am. Chem. Soc.* **1938**, *60* (1), 309–319. https://doi.org/citeulike-article-id:4074706\rdoi:

10.1021/ja01269a023.

(38) Mehlich, A. Mehlich 3 Soil Test Extractant: A Modification of Mehlich 2 Extractant. *Commun. Soil Sci. Plant Anal.* **1984**, *15* (12), 1409–1416. https://doi.org/10.1080/00103628409367568.

(39) J. Matula. *A Relationship between Multi-Nutrient Soil Tests (Mehlich 3, Ammonium Acetate, and Water Extraction) and Bioavailability of Nutrients from Soils for Barley*.

(40) Das, S. K.; Ghosh, G. K.; Avasthe, R. Evaluating Biomas-Derived Biochar on Seed Germination and Early Seedling Growth of Maize and Black Gram. *Biomass Convers. Biorefinery* **2020**, 1–14. https://doi.org/10.1007/s13399-020-00887-8.

(41) Method 3540C, Revision III. *Final Updat. III to Third Ed. Test Methods Eval. Solid Waste, Phys. Methods, EPA Publ. SW-846. (5)2*.

(42) Cao, Y.; Wang, K.; Wang, X.; Gu, Z.; Ambrico, T.; Gibbons, W.; Fan, Q.; Talukder, A.-A. Preparation of Active Carbons from Corn Stalk for Butanol Vapor Adsorption ☆. *J. Energy Chem.* **2017**, *26*, 35–41. https://doi.org/10.1016/j.jechem.2016.08.009.

(43) IBI. *Standardized Product Definition and Product Testing Guidelines for Biochar That Is Used in Soil (Aka IBI Biochar Standards)*; 2015.

(44) Lu, H. R.; Hanandeh, A. El. Life Cycle Perspective of Bio-Oil and Biochar Production from Hardwood Biomass; What Is the Optimum Mix and What to Do with It? **2018**. https://doi.org/10.1016/j.jclepro.2018.12.025.

(45) Yue, Y.; Cui, L.; Lin, Q.; Li, G.; Zhao, X. Efficiency of Sewage Sludge Biochar in Improving Urban Soil Properties and Promoting Grass Growth. *Chemosphere* **2017**, *173*, 551–556. https://doi.org/10.1016/j.chemosphere.2017.01.096.

(46) Bruno Glaser, J. L. W. Z. Ameliorating Physical and Chemical Properties of Highly Weathered Soils in the Tropics with Charcoal – a Review. *Biol Fertil Soils* **2002**. https://doi.org/10.1007/s00374-002-0466-4.

(47) Saifullah; Dahlawi, S.; Naeem, A.; Rengel, Z.; Naidu, R. Biochar Application for the Remediation of Salt-Affected Soils: Challenges and Opportunities. *Sci. Total Environ.* **2018**, *625*, 320–335. https://doi.org/10.1016/j.scitotenv.2017.12.257.

(48) Forján, R.; Asensio, V.; Rodríguez-Vila, A.; Covelo, E. F. Effect of Amendments Made of Waste Materials in the Physical and Chemical Recovery of Mine Soil. **2014**. https://doi.org/10.1016/j.gexplo.2014.10.004.

(49) Laird, D.; Flemming, P.; Wang, B.; Horton, R.; Karlen, D. Biochar Impact on Nutrient Leaching from a Midwestern Agricultural Soil. **2010**. https://doi.org/10.1016/j.geoderma.2010.05.012.

(50) Chatterjee, R.; Sajjadi, B.; Chen, W. Y.; Mattern, D. L.; Hammer, N.; Raman, V.; Dorris, A. Effect of Pyrolysis Temperature on PhysicoChemical Properties and Acoustic-Based Amination of Biochar for Efficient CO2 Adsorption. *Front. Energy Res.* **2020**, *8*. https://doi.org/10.3389/fenrg.2020.00085.

(51) Berger, M.; Ford, J.; Goldfarb, J. L. Modeling Aqueous Contaminant Removal Due to Combined Hydrolysis and Adsorption: Oxytetracycline in the Presence of Biomass-Based Activated Carbons. *Sep. Sci. Technol.* **2018**, 1–17. https://doi.org/10.1080/01496395.2018.1520721.

(52) Senthilkumar, R.; Mogili Reddy Prasad, D. Sorption of Heavy Metals onto Biochar. In *Applications of Biochar for Environmental Safety [Working Title]*; IntechOpen, 2020. https://doi.org/10.5772/intechopen.92346.

(53) Rengga, W. D. P.; Sudibandriyo, M.; Nasikin, M. Development of Formaldehyde Adsorption Using Modified Activated Carbon -A Review. *J. Renew. Energy Dev.* **2012**, *1* (3), 80.

(54) Wan Mahari, W. A.; Nam, W. L.; Sonne, C.; Peng, W.; Phang, X. Y.; Liew, R. K.; Yek, P. N. Y.; Lee, X. Y.; Wen, O. W.; Show, P. L.; et al. Applying Microwave Vacuum Pyrolysis to Design Moisture Retention and PH Neutralizing Palm Kernel Shell Biochar for Mushroom Production. *Bioresour. Technol.* **2020**, *312*, 123572. https://doi.org/10.1016/j.biortech.2020.123572.

(55) Liew, R. K.; Chai, C.; Yek, P. N. Y.; Phang, X. Y.; Chong, M. Y.; Nam, W. L.; Su, M. H.; Lam, W. H.; Ma, N. L.; Lam, S. S. Innovative Production of Highly Porous Carbon for Industrial Effluent Remediation via Microwave Vacuum Pyrolysis plus Sodium-Potassium Hydroxide Mixture Activation. *J. Clean. Prod.* **2019**, *208*, 1436–1445. https://doi.org/10.1016/j.jclepro.2018.10.214.

(56) Ge, S.; Foong, S. Y.; Ma, N. L.; Liew, R. K.; Wan Mahari, W. A.; Xia, C.; Yek, P. N. Y.; Peng, W.; Nam, W. L.; Lim, X. Y.; et al. Vacuum Pyrolysis Incorporating Microwave Heating and Base Mixture Modification: An Integrated Approach to Transform Biowaste into Eco-Friendly Bioenergy Products. *Renew. Sustain. Energy Rev.* **2020**, *127*, 109871. https://doi.org/10.1016/j.rser.2020.109871.